J Seismol
DOI 10.1007/s10950-016-9558-8

ORIGINAL ARTICLE

Reconditioning fault slip inversions via InSAR data discretization

Alon Ziv

Received: 29 September 2015 / Accepted: 27 January 2016

Abstract A major difficulty in inverting geodetic data for fault slip distribution is that measurement errors are mapped from the data space onto the solution space. The amplitude of this mapping is sensitive to the condition number of the inverse problem, i.e., the ratio between the largest and smallest singular value of the forward matrix. Thus, unless the problem is well-conditioned, slip inversions cannot reveal the actual fault slip distribution. In this study, we describe a new iterative algorithm that optimizes the condition of the slip inversion through discretization of InSAR data. We present a numerical example that demonstrates the effectiveness of our approach. We show that the condition number of the reconditioned data sets are not only much smaller than those of uniformly spaced data sets with the same dimension but are also much smaller than non-uniformly spaced data sets, with data density that increases towards the model fault.

Keywords Earthquake seismology · Inversion · Coseismic slip · InSAR

A. Ziv (✉)
Department of Geosciences, Tel-Aviv University,
Ramat-Aviv, Tel-Aviv 69978, Israel
e-mail: zivalon@tau.ac.il

1 Introduction

Since the advent of InSAR and its first application to the mapping of ground displacement in the 1990s (Massonnet et al. 1993), dense line of sight (LOS) displacement data are being routinely inverted for fault slip distributions. An important step in those slip inversions is the discretization of the InSAR data. Apart from reducing the size of the data while preserving the important information (Simons et al. 2002; Jónsson et al. 2002; Lasserre et al. 2005; Lohman and Simons 2005; Grandin et al. 2009), the data discretization should be done in a manner that reduces the sensitivity of the resulting slip distribution to small variations in the data.

The slip distribution is solved on a set of rectangular or triangular elastic dislocations, and the forward relation between the modeled slip, m, and the LOS displacement data, d, is:

$$Gm = d, \tag{1}$$

where G is the elasto-static kernel. In cases where the deformation source is deep, the spatial gradient of the data vector is expected to be moderate, and use of a uniform spacing between data points is appropriate. Otherwise, for shallow deformation sources, the ground displacement gradient may be strong, and it is important to employ a non-uniform spacing. Previous

Published online: 11 February 2016

approaches for non-uniform InSAR data discretization were based either on the spatial variations in d (e.g., Simons et al. 2002; Jónsson et al. 2002; Funning et al. 2007) or a resolution analysis of G (Lohman and Simons 2005). Data space discretizations that use variations in the data vector rest on the assumption that areas of strong surface deformation (or deformation gradient) reflect deformation in the source, and result in highest density of data points in areas of strong ground displacement. Lohman and Simons (2005) pointed out that since some of the variability in the data space is due to atmospheric noise, errors in the satellite orbit and analysis errors, these artifacts may affect the solution. To avoid data oversampling in noisy areas, Wang and Fialko (2015) implemented an iterative downsampling algorithm that uses the phase gradient predicted by the best fitting model.

The data space is "contaminated" with noise and errors of various sources, and these may introduce spurious structures in the slip model. Thus, when designing an inverse problem, one should verify that the problem is well-conditioned, i.e., that small changes in the data space do not cause large changes in the model space. In this study, we describe a new algorithm for InSAR data discretization that optimizes the condition of the inverse problem, and present a numerical example that demonstrates the effectiveness of our approach.

2 Method

2.1 The objective function

The assessment of the problem condition begins with the singular value decomposition (SVD) of G, to get: $G = U\Sigma V^T$, where U is an orthonormal matrix of eigenvectors that span the data space, V is an orthonormal matrix of eigenvectors that span the model space, and Σ is a diagonal matrix $\Sigma = (\sigma_1, \ldots, \sigma_n)$ with $\sigma_1 \geq \sigma_2 \geq \ldots \geq \sigma_n \geq 0$ being the singular values of G, whose dimension equals n. Following SVD, the generalized inverse of G is:

$$G^{-g} = V\Sigma^{-1}U^T. \tag{2}$$

If noise and measurement errors are included, the forward relation in Eq. 1 becomes:

$$Gm + d_{err} = d. \tag{3}$$

From Eqs. 2 and 3, the presence of noise introduces model errors according to:

$$m_{err} = V\Sigma^{-1}U^T d_{err}, \tag{4}$$

which shows that errors in the data space are mapped into the solution parallel to each eigenvector in V, with an amplification factor $1/\sigma$ corresponding to that eigenvector. Thus, very small singular values render the solution unstable and unreliable (Menke 1989), and it makes sense to make the magnitude of the smallest singular value in the spectrum of G as large as possible (Barth and Wunsch 1990; Curtis and Snieder 1997). Therefore, the objective function that we seek to minimize is the condition number (e.g., Goulb and Van Loan 1996):

$$CN = \frac{\sigma_1}{\sigma_n}, \tag{5}$$

where σ_1 and σ_n are the first (largest) and last (smallest) singular values, respectively. The smaller the condition number, the larger the rank of G, the smaller the null space and the better the condition of the inverse problem (Barth and Wunsch 1990). Below, we present a new iterative algorithm for InSAR data discretization that optimizes the condition of the inverse problem.

2.2 The algorithm

The data discretization algorithm proceeds along the following steps:

1. Setup a pre-determined model fault geometry.
2. Setup a starting set of uniformly spaced data points. The size of the starting data set is chosen such that the inverse problem is slightly overdetermined.
3. Iterate over all data points, and for each:
   (a) Perform a quad-division and replace that point with a set of four new data points
   (b) Recalculate a new elastic kernel, G.
   (c) Compute the SVD of G.
   (d) Compute and store the condition number CN_i, with i being the index of the data point in question.
4. Extract the subset of data points whose condition number is amongst the lowest 5 %, and form a new data set by replacing each such data point by four new data points obtained through a quad-division.

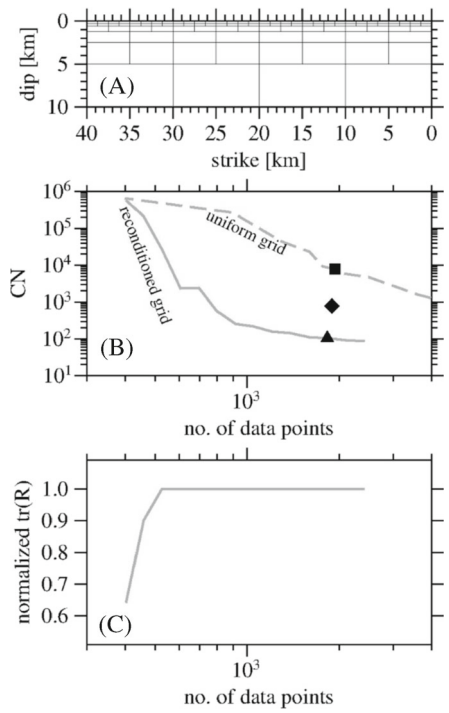

Fig. 1 Results of synthetic data discretization. **a** The predetermined fault discretization used in this study. **b** The condition number as a function of the number of data points. Results for the reconditioned and uniformly-spaced grids are shown in *solid* and *dashed curves*, respectively. The *three solid symbols* correspond to the three data distribution maps shown in Fig. 2. **c** The trace of the resolution matrix normalized by the model size as a function of the number of data points. Values close to a unity indicate perfectly determined models. Note that an inverse problem can be poorly conditioned (i.e., large CN) despite the model being perfectly determined

5. Repeat steps 3 and 4, or quit after verifying that further increasing the number of data points does not improve the condition number.

In reality, some of the data are missing due to phase decorrelation, and it is sensible to weight each entry in G in proportion to the fraction of valid data points within the data quad corresponding to that entry.

3 Numerical examples

Results presented here were calculated for a vertical strike-slip fault striking at an azimuth of 80° with respect to the satellite orbit and discretized into 100 rectangular dislocations (Okada 1985) as shown in Fig. 1a. The starting data set consisted of 20 by 20 uniformly spaced data points. The CN as a function of

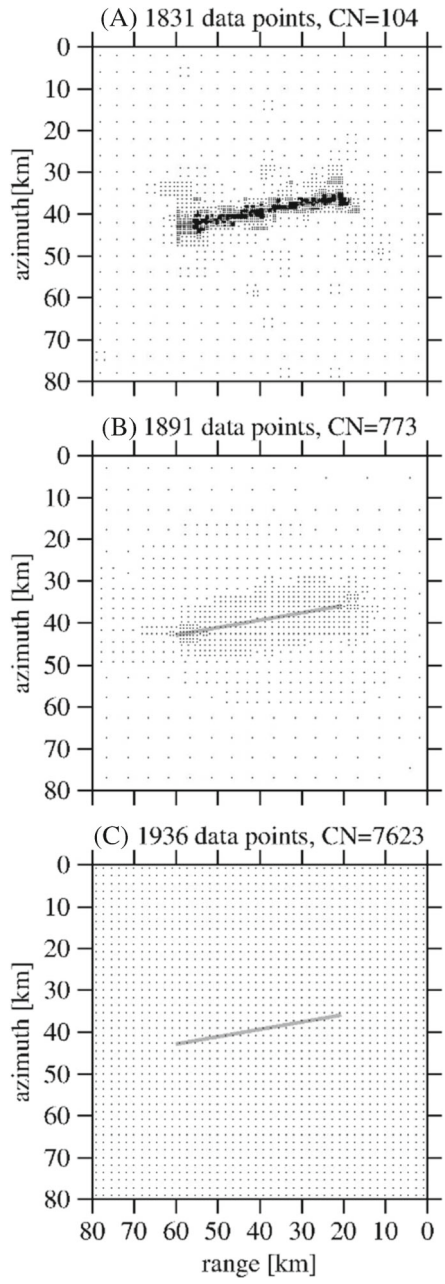

Fig. 2 The three data grids used for the error sensitivity analyses (whose results are summarized in Figs. 3 and 4). **a** Reconditioned grid. **b** A data grid whose spacing is proportional to the variance of the LOS displacement due to the model fault slipping uniformly by 0.5 m. **c** A uniformly spaced data grid. The number of data points and the value of CN corresponding to each grid are indicated

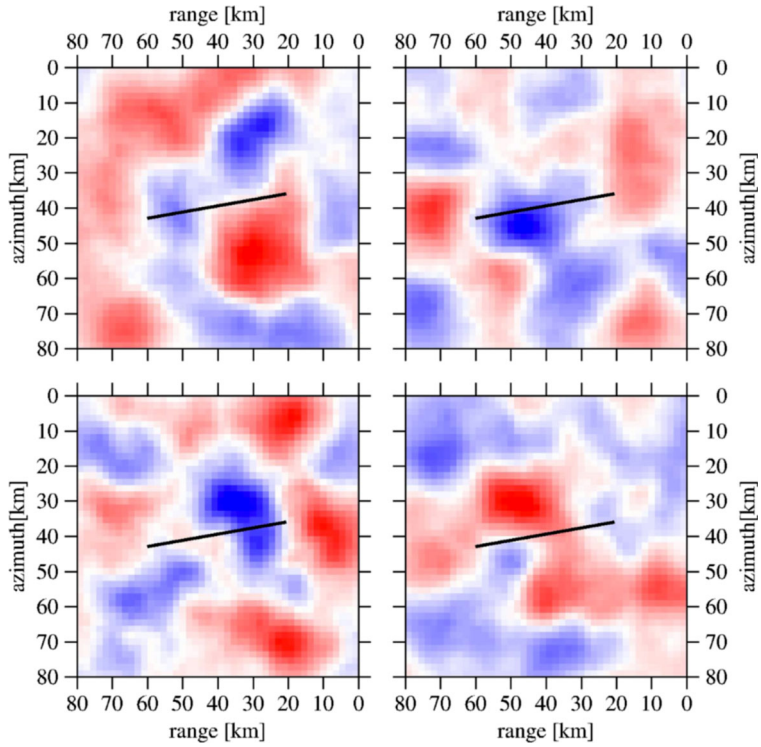

Fig. 3 Representative examples of the spatially-correlated noise used in this study. The mean and maximum absolute values are zero and 1 cm, respectively

the number of data points is shown in Fig. 1b. Increasing the data set from 400 to 2000 data points results in four orders of magnitude decrease in the condition number. Beyond that point, however, the condition number curve becomes nearly flat. In Fig. 2a, we show a reconditioned data set consisting of about 1800 data points (corresponding to the solid triangle in Fig. 1b). Clearly, this data distribution map differs markedly from what one would obtain through application of the previously used data downsampling methods (Simons et al. 2002; Jónsson et al. 2002; Lohman and Simons 2005).

In order to assess the extent to which our algorithm improves the condition of the inverse problem, we compare the CN of reconditioned data configurations with those of uniformly spaced data sets (dashed curve in Fig. 1b). We find that the condition numbers of the reconditioned data configurations are much smaller than those of uniformly spaced data of similar size. For example, the CN of a reconditioned data configuration consisting of 1831 data points (Fig. 2a) and a uniformly distributed data set consisting of 1936 data points (Fig. 2c) are equal to 104 and 7623, respectively. Furthermore, we computed the CN of a data grid, whose density increases proportionally to the gradient of the LOS displacement resulting from the entire model fault slipping uniformly by 0.5 m (Fig. 2b), and found that it is by a factor of 7 larger than that of the reconditioned grid. We thus conclude that the condition number of reconditioned data grids is not only much smaller than those of uniformly spaced data sets with the same dimension, but are also much smaller than non-uniformly spaced data sets, with data density that increases toward the fault trace.

The errors in the final model due to random errors in the data were quantified using a Monte Carlo procedure. We generated a synthetic LOS displacement distribution, and used that as our error-free data set. Next, we generated 1000 perturbed data sets by adding randomly generated number to each of the error-free data point. We consider two types of random errors, a spatially-uncorrelated normally distributed random number with a zero mean and a spatially-correlated noise with a zero mean and maximum absolute amplitude of 1 cm (Fig. 3). In addition, we consider two slip distributions that may be regarded as end-members with respect to their slip variability. In the first, the synthetic LOS displacement is

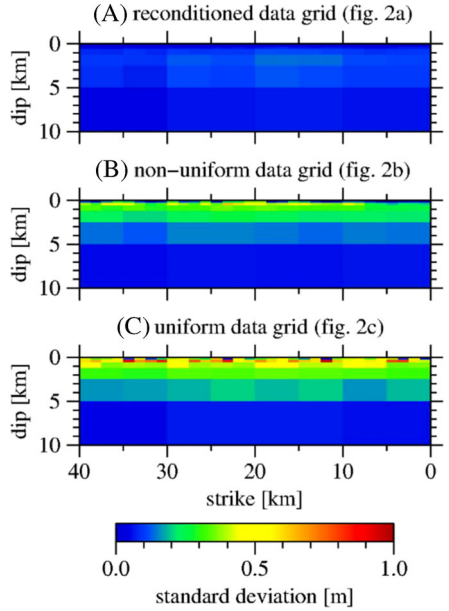

Fig. 4 Sensitivity to spatially uncorrelated random data errors (standard deviation of 5 mm) of a fault slipping uniformly by 0.5 m. The standard deviation of 1000 slip inversions are shown for **a** reconditioned data grid, **b** a grid whose spacing is proportional to the variance of the LOS displacement, and **c** a uniform grid. The number of data points and CN of each grid are indicated in Fig. 2

due to the entire model fault slipping uniformly by 0.5 m, and in the second the LOS displacement is due to the model fault slipping randomly between 0 and 1 m. We then used the nonnegative least squares algorithm of Lawson and Hanson (1974) to invert each of the perturbed data set. After obtaining a suite of 1000 slip models, we computed the average modeled slip and the standard deviation of the discrepancies between the modeled and the true (i.e., input) slip on each of the 100 dislocations comprising the model fault.

The results for the spatially-uncorrelated random noise are summarized in Figs. 4 and 5, and those for the spatially-correlated noise are shown in Fig. 6. Inspection of the standard deviation of the slip discrepancies associated with the three data maps in these figures reveals a clear reduction in the slip discrepancy with decreasing condition number. Thus, use of our data discretization scheme successfully reduces the effect of noise. While the standard deviation of the slip discrepancies are very sensitive to the choice of the data discretization, the average modeled slip is not and is nearly identical to the input slip distribution (left-hand panels in Fig. 5). We wish to emphasize that in contrast to the common practice in fault slip inversions, we did not impose any smoothing on the solutions. Yet, despite the omission of the smoothing constraint, we are able to recover similarly well the input slip distributions of the two tests.

As mentioned previously, minimizing CN reduces the quasi-null space of the inverse problem, i.e., the number of very small eigenvalues, and guarantees that the problem is fully determined (Barth and Wunsch 1990). A quantity that measures the number of linearly independent parameters is the trace of the resolution matrix, R, given by: $tr(R) = tr(GG^{-g})$.

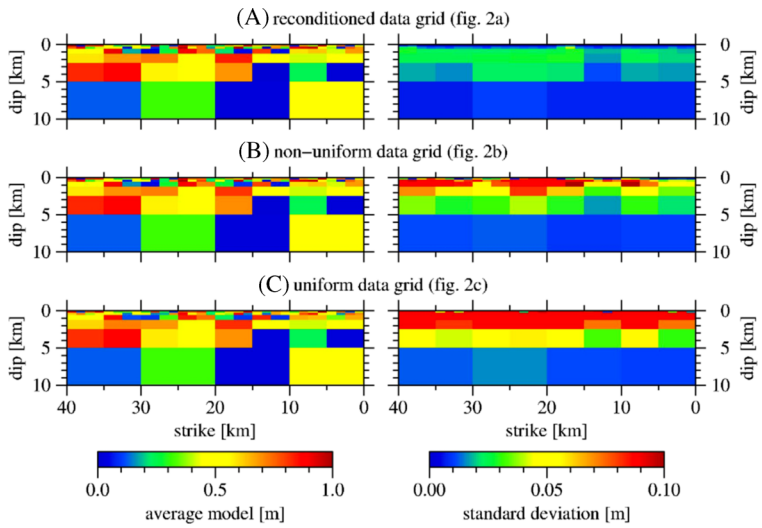

Fig. 5 Sensitivity to spatially uncorrelated random data errors (standard deviation of 1 mm) of a fault with random slip distributed uniformly between 0 and 1 m. The average slip (*left-hand panels*) and the slip standard deviation (*right-hand panels*) of 1000 inversions are shown for **a** reconditioned data grid, **b** a grid whose spacing is proportional to the variance of the LOS displacement, and **c** a uniform grid. The number of data points and CN of each grid are indicated in Fig. 2

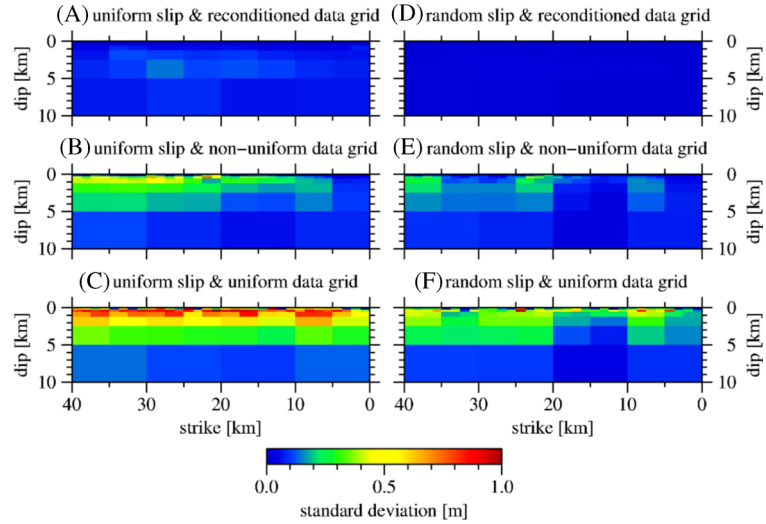

Fig. 6 Sensitivity to spatially correlated random data errors. The standard deviation of 1000 slip inversions are shown for **a** reconditioned data grid and a fault slipping uniformly by 0.5 m, **b** a grid whose spacing is proportional to the variance of the LOS displacement and a fault slipping uniformly by 0.5 m, **c** a uniform grid and a fault slipping uniformly by 0.5 m, **d** reconditioned data grid and a fault slipping randomly between 0 and 1 m, **e** a grid whose spacing is proportional to the variance of the LOS displacement and a fault slipping randomly between 0 and 1 m, and **f** a uniform grid and a fault slipping randomly between 0 and 1 m. The number of data points and CN of each grid are indicated in Fig. 2

The closer this quantity to the model size, the better the model resolution. In Fig. 1c, we show normalized $tr(R)$ (i.e., divided by the model size) as a function of the number of data points. We find that the reconditioned data grids are fully determined for data sets greater than about 500 data points. This shows that an inverse problem can be poorly conditioned despite the model being perfectly determined, and further highlights the advantage of the conditioning optimization over resolution-based optimization algorithms.

4 Summary and conclusions

We described a simple algorithm for dense geodetic data discretization for fault slip inversion, whose objective function is the condition number of the matrix G in Eq. 1. Minimizing the condition number is equivalent to minimizing of the null space of the inverse problem, and has the effect of stabilizing the solution with respect to small changes in the data.

We showed that the condition number of reconditioned data grids are not only much smaller than those of uniformly spaced data sets with the same dimension but are also much smaller than non-uniformly spaced data sets, with data density that increases towards the fault trace. We presented the results of Monte Carlo tests, illustrating the reduction in model errors (due to noise added to the data space) with decreasing condition number. We thus conclude that use of the reconditioning scheme can improve the accuracy and the reliability of slip models.

Our algorithm takes as an input a pre-determined fixed model configuration. Rather than fixing the model configuration and discretizing the data space, one could fix the distribution of the data points and parameterize the model space (e.g., Page et al. 2009; Barnhart and Lohman 2010). It is worth noting that the approach for optimizing the condition of the slip inversion described in this study, with only slight modifications to our algorithm, may also be implemented for the parameterization of the model space.

In summary, optimizing the condition of inverse problems is an effective technique for reducing the effect of noise and analysis errors. Unless the inverse problem is well-conditioned, slip inversions cannot reveal the actual fault slip distribution.

Acknowledgments I thank the associate editor, Shamita Das, for her work. Comments and suggestions from two anonymous reviewers helped to improve the manuscript.

References

Barnhart WD, Lohman RB (2010) Automated fault model discretization for inversions for coseismic slip distributions. J Geophys Res 115:B10419. doi:10.1029/2010JB007545

Barth N, Wunsch C (1990) Oceanographic experiment design by simulated annealing. J Phys Oceanography 20:1249–1263

Curtis A, Snieder R (1997) Reconditioning inverse problems using the genetic algorithm and revised parameterization. Geophysics 62(4):1524–1532

Funning GJ, Bürgmann R, Ferretti A, Novali F, Fumagalli A (2007) Creep on the Rodgers Creek fault, northern San Francisco Bay area, from a 10-year PS-inSAR dataset. Geophys Res Lett 34:L19306. doi:10.1029/2007GL030836

Goulb GH, Van Loan CF (1996) Matrix computation. The John Hopkins University Press, Baltimore and London

Grandin R, Socquet A, Binet R, Klinger Y, Jacques E, de Chabalier JB, King GCP, Lasserre C, Tait S, Tapponnier P, Delorme A, Pinzuti P (2009) September 2005 Manda Hararo-Dabbahu rifting event, Afar (Ethiopia): constraints provided by geodetic data. J Geophys Res 114:B08404. doi:10.1029/2008JB005843

Jónsson S, Zebker H, Segall P, Amelung F (2002) Fault slip distribution of the 1999 mw 7.1 Hector Mine, California, earthquake, estimated from satellite radar and GPS measurements. Bull Seism Soc Am 92:1377–1389

Lasserre C, Peltzer G, Crampe F, Klinger Y, Van der Woerd J, Tapponnier P (2005) Coseismic deformation of the 2001 Mw = 7.8 Kokoxili earthquake in Tibet, measured by synthetic aperture radar interferometry. J Geophys Res 110:B12408. doi:10.1029/2004JB003500

Lawson CL, Hanson BJ (1974) Solving least squares problems. Prentice-Hall Inc., Englewood Cliffs

Lohman RB, Simons M (2005) Some thoughts on the use of inSAR data to constrain models of surface deformation: noise structure and data downsampling. Geochem Geophys Geosyst 6:Q01007. doi:10.1029/2004GC000841

Massonnet D, Rossi M, Carmona C, Adragna F, Peltzer G, Feigl K, Rabaute T (1993) The displacement field of the Landers earthquake mapped by radar interferometry. Nature 364:138–142

Menke W (1989) Geophysical data analysis: discrete inverse theory, Vol 45 of international geophysics series. Academic Press, San Diego

Okada Y (1985) Surface deformation due to shear and tensile faults in a half-space. Bull Seism Soc Am 75:1135–1154

Page MT, Custódio S, Archuleta RJ, Carlson JM (2009) Constraining earthquake source inversions with GPS data: 1. Resolution-based removal of artifacts. J Geophys Res 114:B01314. doi:10.1029/207JB005449

Simons M, Fialko Y, Rivera L (2002) Coseismic deformation from the 1999 Mw 7.1 Hector Mine, California, earthquake as inferred from InSAR and GPS observations. Bull Seism Soc Am 92:1390–1402

Wang K, Fialko Y (2015) Slip model of the 2015 Mw7.8 Gorkha (Nepal) earthquakefrom inversions of ALOS-2 and GPS data. Geophys Res Lett 42:7452–7458. doi:10.1002/2015GL065201